Transmembrane and coiled-coil domain 1 impairs the AKT signaling pathway in urinary bladder urothelial carcinoma: a characterization of a tumor suppressor

Chien-Feng Li[1,2,3,4], Wen-Ren Wu[5], Ti-Chun Chan[1,5], Yu-Hui Wang[1,6], Lih-Ren Chen[4,7,8], Wen-Jeng Wu[9,10,11,12,13,14,15], Bi-Wen Yeh[9], Shih-Shin Liang[5,16], Yow-Ling Shiue[5,17,18,*]

[1]Department of Pathology, Chi Mei Medical Center, Tainan, Taiwan. [2]Natioanl Institute of Cancer Research National Health Research Institute, Tainan, Taiwan. [3]Department of Pathology Kaohsiung Medical University, Kaohsiung, Taiwan. [4]Department of Biotechnology, Southern Taiwan University of Science and Technology, Tainan, Taiwan. [5]Institute of Biomedical Sciences, National Sun Yat-sen University, Kaohsiung, Taiwan. [6]Institute of Bioinformatics and Biosignal Transduction, National Cheng Kung University, Tainan, Taiwan. [7]Division of Physiology, Livestock Research Institute, Council of Agriculture, Taiwan. [8]Institute of Biotechnology, National Cheng Kung University, Tainan, Taiwan. [9]Department of Urology, Kaohsiung Medical University Hospital, Kaohsiung, Taiwan. [10]Department of Urology, School of Medicine, College of Medicine, Kaohsiung Medical University, Kaohsiung, Taiwan. [11]Graduate Institute of Medicine, College of Medicine, Kaohsiung Medical University, Kaohsiung, Taiwan. [12]Center for Infectious, Disease and Cancer Research, Kaohsiung Medical University, Kaohsiung, Taiwan. [13]Center for Stem Cell Research, Kaohsiung Medical University, Kaohsiung, Taiwan. [14]Department of Urology, Kaohsiung Municipal Ta-Tung Hospital, Kaohsiung, Taiwan. [15]Institute of Medical Science and Technology, Kaohsiung Medical University, Kaohsiung, Taiwan. [16]Department of Biotechnology, Kaohsiung Medical University, Kaohsiung, Taiwan. [17]Department of Biological Sciences, National Sun Yat-sen University, Kaohsiung, Taiwan. [18]Doctoral degree program in Marine Biotechnology, National Sun Yat-sen University, Kaohsiung, Taiwan

Running title: TMCO1 is a tumor suppressor in UBUCs

Keywords: TMCO1, AKT, urinary bladder urothelial carcinoma, tumor suppressor

***Corresponding author:** Yow-Ling Shiue, PhD, Institute of Biomedical Sciences, National Sun Yat-sen University, 70 Lienhai Road, 80424 Kaohsiung, Taiwan. Phone: 886-7-5255818; Fax: 886-7-5250197; Email: shirley@imst.nsysu.edu.tw

Conflict of interest: the authors declare no conflicts of interest

Grand support: Li, CF was funded by Ministry of Health and Welfare (MOHW105-TDU-B-212-134007) and Ministry of Science and Technology (MOST104-2314-B-037-050-MY3). Wu, WJ was supported by Kaohsiung Medical University 'Aim for the Top Universities" (KMU-TP105G00, KMU-TP105G01, KMU-TP105G02), Center for Infectious Disease and Cancer Research (KMU-TP105E24), Kaohsiung Medical University Research Foundation (KMUOR105), NSYSU-KMU Joint Research Project (NSYSUKMU 106-P008). It is also supported by Kaohsiung Medical University Hospital (KMUH104-4R44, KMUH105-5R47) and Ministry of Science and Technology (MOST104-2314-B-037-050-MY3). Both Li, CF and Wu, WJ were supported by the health and welfare surcharge on tobacco products, Ministry of Health and Welfare (MOHW106-TDU-B-212-144007). Shiue, YL was funded by (MOST105-2314-B-110 -002 -MY2) and the Taiwan Protein Project (MOST105-0210-01-12-01 and MOST106-0210-01-15-04).

Translational Relevance

Urinary bladder urothelial carcinoma (UBUC) is a common malignant disease, especially in developed countries. Almost 50% of patients eventually progress and develop systemic disease. Cell cycle dysregulation resulting in uncontrolled cell proliferation has been associated with UBUC development. Thus, restoring the function of a critical molecule is a rational approach for UBUC treatment. In this study, we performed data mining and identified a potential tumor suppressor, *TMCO1*, in UBUCs. Clinical associations, xenograft mice and in vitro indications from distinct UBUC-derived cell lines provided strong evidence that the *TMCO1* gene is a novel tumor suppressor via the inhibition of the AKT signaling pathway. Downregulation of the TMCO1 protein can be used as an adverse prognostic factor for inferior outcomes in UBUC patients. Our findings provide important insights into the mechanisms of UBUC development and highlight the potential targets for therapeutic interventions.

Purpose: Urinary bladder urothelial carcinoma (UBUC) is a common malignant disease in developed countries. Cell cycle dysregulation resulting in uncontrolled cell proliferation has been associated with UBUC development. This study aimed to explore the roles of *TMCO1* in UBUCs.

Experimental Design: Data mining, branched DNA assay, immunohistochemistry, xenograft, cell culture, quantitative RT-PCR, immunoblotting, stable and transient transfection, lentivirus production and stable knockdown, cell cycle, cell viability and proliferation, soft agar, wound healing, transwell migration and invasion, co-immunoprecipitation, immunocytochemistry, AKT serine/threonine kinase (AKT) activity assays and site-directed mutagenesis were used to study *TMCO1* involvement in vivo and in vitro.

Results: Data mining identified that the *TMCO1* transcript was downregulated during the progression of UBUCs. In distinct UBUC-derived cell lines, changes in TMCO1 levels altered the cell-cycle distribution, cell viability, cell proliferation, colony formation and modulated the AKT pathway. TMCO1 recruited the PH domain and leucine rich repeat protein phosphatase 2 (PHLPP2) to dephosphorylate pAKT1(serine 473) (S473). Mutagenesis at S60 of the TMCO1 protein released TMCO1-induced cell cycle arrest and restored the AKT pathway in BFTC905 cells. Stable *TMCO1* (wild-type) overexpression suppressed, while T33A and S60A mutants recovered, tumor size in xenograft mice.

Conclusions: Clinical associations, xenograft mice and in vitro indications provide solid evidence that the *TMCO1* gene is a novel tumor suppressor in UBUCs. TMCO1 dysregulates cell cycle progression via suppression of the AKT pathway, and S60 of the TMCO1 protein is crucial for its tumor suppressor roles.

Introduction

Urinary bladder urothelial carcinoma (UBUC) is a common malignant disease, especially in developed countries (1). Both environmental and genetic factors impact UBUC development (2,3). Clinicopathological features, including histological grade, stage, size and multiplicity, are associated with its progression (4). Despite improvements in surgical techniques and multimodal therapy, 5-year survival rates for patients with muscle-invasive UBUC remain suboptimal. Almost 50% of patients eventually progress and develop systemic disease (5). Clinical and genetic heterogeneity observed in UBUC patients further complicates the use of general therapies (6). Cell cycle dysregulation resulting in uncontrolled cell proliferation has been associated with UBUC development (7,8). Thus, targeting a critical molecule for therapies is a rational approach for UBUC treatment (9).

To identify transcripts that are potentially involved in UBUC development, data mining established expression profiles (GSE31684, $n = 93$) in the Gene Expression Omnibus database (GEO, NCBI, Bethesda, MD, USA) was performed. One differentially expressed transcript, transmembrane and coiled-coil domain 1 (*TMCO1*), was identified to be associated with growth factor activity (GO:0008083; molecular function) and was highly expressed in pTa ($P = 0.0006$) and pT1 ($P = 0.0174$), compared to pT2-T4 patients with UBUC. The human *TMCO1* gene, mapped to human chromosome 1q24.1, encodes a transmembrane protein (10), is a member of the DUF841 superfamily of several eukaryotic proteins with unknown function or involvement in any biological process (11). The 3D structure of TMCO1 protein has not be resolved, yet its topology contains 2 transmembrane domains (#10-30; #91-111) and 1 intramembrane fragment (#138-154) (12). Green fluorescent protein-tagged and Myc-tagged TMCO1 were found to be expressed in the endoplasmic reticulum (ER) and/or the Golgi apparatus of COS7 and HeLa cells (12,13). *TMCO1* mRNA is highly expressed in porcine heart, liver and kidney (14). Data mining, and the fact that

membrane proteins constitute the largest class of drug targets (15), prompted us to systematically analyze the relevance of TMCO1 immunoexpression and clinicopathological features in UBUC patients and its biological significance in vitro and in vivo.

Materials and Methods

Data mining, patients, tumor materials and immunohistochemistry

The procedure for data mining the GEO database to identify downregulated transcripts in UBUCs is described in the Supplementary Materials and Methods. For immunohistochemistry, the institutional review board of Chi Mei Medical Center approved the retrospective retrieval of 295 primary UBUCs with available tissue blocks (IRB10207-001), which underwent surgical treatment with curative intent between January 1998 and May 2004. These patients received surgical resection with curative intent between 1998 and 2004, while those who underwent palliative resection were excluded. Patients with confirmed or suspected lymph node metastasis received regional lymph node dissection. Cisplatin-based post-operative adjuvant chemotherapy was performed in patients with pT3-pT4 status or nodal involvement. The histological diagnosis of UBUCs was confirmed in all cases based on the latest World Health Organization classification. Histological grading was assigned on the basis of Edmonson-Steiner criteria, while tumor staging was determined according to the 7th edition of the American Joint Committee on Cancer system. Medical charts were reviewed for each patient to ascertain the accuracy of other pertinent clinicopathological data. Follow-up information was available in all cases with a median period of 42 months (ranging 3-176 months). To determine the clinical relevance of the *TMCO1* transcript level, an independent cohort comprised of 15 pTa-T1 and 15 pT2-T4 tumors and 9 non-tumor urothelial samples were enrolled and evaluated by branched DNA assay. Immunohistochemical staining was performed on representative tissue sections cut

from formalin-fixed, paraffin-embedded tissues at 3-μm thickness as in our previous study (16) with a few modifications (Supplementary Materials and Methods).

Cell culture and chemicals

Human normal urothelial cells (HUC; #4320, ScienCell Research Laboratories) were obtained and cultured with the recommended medium (#4321, ScienCell Research) in poly-L-lysine coated flasks (2 $\mu g/cm^2$). The human UBUC-derived cell lines RT4 (Food Industry Research and Development Institute, Hsinchu, Taiwan), J82 (ATCC), T24 (ATCC), and BFTC905 and BFTC909 (kindly provided by Dr. Tzeng CC) (17) were respectively maintained in McCoy's 2A, DMEM, DMEM, RPMI-1640 and DMEM supplemented with 10% (v/v) fetal bovine serum (Biological Industries), appropriate nutrients and antibiotics in a humidified incubator with 5% CO_2 at 37°C. All media were obtained from CORNING. RT4 (18) and BFTC905 (19) were characterized with wild-type TP53; however, J82 was an allele-specific mutation of TP53 (20). The pan-PH domain and leucine rich repeat protein phosphatase (PHLPP) inhibitor, NSC117079 [1-amino-9,10-dioxo-4-(3-sulfamoylanilino)anthracene-2-sulfonic acid], was obtained from AOBIOUS (Gloucester, MA, USA). All cell lines were authenticated by short tandem repeat genotyping, periodically confirmed to be mycoplasma-free using PlasmoTest™ (Invivogen) in IMDM (Invitrogen) supplemented with 15% fetal bovine serum, 100 U/mL.

Quantitative RT-PCR and immunoblot analysis

Quantitative RT-PCR assay was applied to quantify the expression levels of several transcripts using predesigned TaqMan® assay reagents, including *TMCO1* (Hs00976965_m1, 123 bp), tumor protein p53 (*TP53*; Hs01034249_m1, 108 bp) and glyceraldehyde-3-phosphate dehydrogenase (*GAPDH*; Hs03929097_g1, 58 bp, internal

control), along with a LightCycler® (Roche Life Science) and $\Delta\Delta C_T$ calculation (21). Immunoblot analyses were performed as in our previous study (Supplementary Materials and Methods).

Expression plasmids, stable and transient transfections

The pCMV6-TMCO1 (RC200219; NM_019026.4) plasmid was purchased from OriGene Technologies. The *TMCO1* complete DNA (564 bp) was subcloned into a pHTC HaloTag® CMV-neo vector (pHaloTag) using 5'-CTAGCTAGCATGAGCACTATGTTCGCGGA-3' and 5'-CCGCTCGAGAGAGAACTTCCCAGAAGGAGGT-3' primers with *Nhe* I and *Xho* I restriction sites (underlined) to generate the pTMCO1-HaloTag plasmid. The pcDNA3-PHLPP2 (#22403) and pHRIG-AKT1 (#53583) plasmids were obtained from Addgene (22,23). All plasmids were sequence verified. Cells (5×10^5) were transfected with 2.5 μg of a specific plasmid by mixing with 7.5 μL of PolyJet™ reagent (SignaGen® Laboratories) in Opti-MEM® (Life Technology). Transfectants were selected with medium containing 800 μg/mL of G418 (AMRESCO) for 7 days and maintained in medium with 400 μg/mL of G418 for subsequent experiments. The same protocol was used for transient transfections without selection by G418.

Lentivirus production and stable knockdown of the *TMCO1* gene

Small hairpin RNA interference (shRNAi) plasmids were inserted into the pLK0.1 vector downstream of the U6 promoter. Clones were obtained from the National RNAi Core Facility, Institute of Molecular Biology, Academia Sinica, Taipei, Taiwan. A total of 5 plasmids targeting *TMCO1* gene were preliminarily screened. The *TMCO1* mRNA levels could be effectively downregulated by only 2 clones. The plasmids shTMCO1#3 (TRCN0000062125: 5'-CCCTAATGGGAATGTTCAATT-3') and shTMCO1#5 (TRCN0000062127:

5'-CATCGAAATCTGCTGGGAGAT-3') were used for knockdown of the *TMCO1* gene, and shLuc (TRCN0000072243:5'-CTTCGAAATGTCCGTTCGGTT-3)' was used as a negative control clone. For stable shRNAi, lentiviral particles were produced. Experimental details are shown in Supplementary Materials and Methods.

Cell cycle, cell viability, proliferation, soft agar, wound healing, transwell migration and transwell invasion assays

Flow cytometric, 3-(4,5-dimethylthiazol-2-yl)-2,5-diphenyltetrazolium bromide (MTT), bromodeoxyuridine (BrdU) and soft agar assays were used to determine alternations of cell cycle distribution, cell viability, cell proliferation and colony formation/anchorage-independent cell growth after the overexpression and knockdown of the *TMCO1* gene in vitro following our previous protocols (21). Cell migration and invasion were analyzed using the wound healing assay and QCM ECMatrix Cell Invasion Kit (ECM554, Millipore). For the above assays, details are described in Supplementary Materials and Methods.

Immunocytochemistry and co-immunoprecipitation

To examine whether TMCO1 colocalizes or interacts with PHLPP1 or PHLPP2, immunocytochemistry and co-immunoprecipitation (co-IP) were performed using our previous procedures (24), and details are described in Supplementary Materials and Methods.

Site-directed mutagenesis

Three plasmids, pTMCO1(T33A)-, pTMCO1(S60A)- and pTMCO1(S84A)-HaloTag with mutations at residues #33, #60 or #84 from threonine/serine to alanine of the TMCO1 protein were constructed using the QuikChange® Lightning Site-Directed Mutagenesis Kit (#210518,

Agilent) and verified by DNA sequencing. The plasmid containing the wild-type *TMCO1* gene, pTMCO1(WT)-HaloTag, served as the template for site-directed mutagenesis on residues T33, S60 and S84 using PCR-based technology. Details of primers sequences are listed in Supplementary Materials and Methods.

AKT activity assay

AKT activity was analyzed by using KinaseSTAR™ Akt Activity Assay Kit (#K435-40, BioVision) according to the manufacturer's instruction. Briefly, BFTC905 cells (5×10^5) were seeded and transfected overnight with pHaloTag, pcDNA3-HA-PHLPP2 and/or 3 *TMCO1*-mutated plasmids. For each assay, 2 μL of AKT-specific antibody was joined to 250 μg protein. Protein A-Sepharose slurry was applied to capture AKT-specific antibody and 2 μL of the recombinant glycogen synthase kinase 3 alpha protein (GSK3A, substrate)/ATP mixture was added. Protein A-Sepharose were subsequently spun down, the supernatant was collected and subjected to immunoblot analysis by probing anti-GSK3A and anti-pGSK3A(S21) antibody.

Tumor xenograft

Animal experiments were approved (#10615) by Affidavit of reviewing of Animal Use Protocol, National Sun Yat-sen University. Cells were implanted into 40 NOD/SCID mice (8 for each group) by subcutaneous injection. BFTC905 cells (1.5×10^7) stably overexpressing either pHaloTag, pTMCO1(WT)-, pTMCO1(T33A)-, TMCO1(S60A)- or TMCO1(S84A)-HaloTag were resuspended in 100 μL of PBS, mixed with 100 μL of matrigel (BD Biosciences) and introduced into the right flank of 7-week-old, male mice. Tumor diameters were measured with a digital caliper every other day, and the tumor volume in mm^3 was calculated as volume = $\pi/6(\text{width})^2 \times \text{length}$. Whole sections from formalin-fixed

xenograft samples were analyzed by immunohistochemistry using pertinent antibodies described in Supplementary Materials and Methods.

Statistics

All calculations were performed using SPSS 14.0 software. To determine the prognostic impact of selected transcripts identified in GSE31684, the deposited cases were subdivided into two clusters based on the expression level of each transcript, detected by a specific probe and computerized by *k*-means clustering ($k = 2$). The survival difference of the two clusters was next calculated by log-rank analysis and plotted using the Kaplan-Meier method for overall survival. The association and comparison between various clinicopathological factors and TMCO1 expression were assessed by the Chi-square test. The endpoint analyzed for survival analysis was disease-specific and metastasis-free survivals. Student's *t*-test was used to examine the significance of differences in fold changes of mRNA levels, cells in different phases of the cell cycle, percentages of cell viability, proliferation and anchorage-independent cell growth. Comparison of xenograft tumor sizes was performed by using one-way ANOVA. For other analyses, two-sided tests of significance were used, and a P value of < 0.05 was considered to be statistically significant.

Results

Data mining identifies that the *TMCO1* transcript is downregulated in the progression of UBUCs, and TMCO1 downregulation confers poor outcomes in UBUC patients

From the transcriptomic profiles of 308 UBUCs deposited in the GEO database using Illumina HumanHT-12 V3.0 Expression BeadChip for analysis, GSE32894, the *TMCO1* transcript was found to be significantly downregulated in muscle-invasive compared to non-muscle-invasive UBUCs (Fig. 1A). In another dataset, GSE31684, which contains 93

UBUC specimens, the downregulation of *TMCO1* transcript predicted inferior overall survival (Fig. 1B and Supplementary Table S1); this result further suggested that the *TMCO1* gene might function as a tumor suppressor in UBUCs. As shown in Fig. 1C, the *TMCO1* mRNA level was highly expressed in non-tumor ($P = 0.001$) and low-stage (pTa-T1; $P = 0.004$), compared to high-stage (pT2-T4) UBUC patients. High TMCO1 expression was also identified in non-tumor urothelium and non-invasive urothelial carcinomas compared to muscle-invasive carcinomas (Fig. 1D). Correlations between TMCO1 expression and various clinicopathological factors are listed in Supplementary Table S2. Univariate log-rank analysis identified that pT, nodal metastasis, histological grade, vascular invasion, perineural invasion, mitotic rate and TMCO1 immunostainings were significantly correlated with disease-specific and metastasis-free survivals in 295 UBUC patients (Table 1). Kaplan-Meier plots revealed that low TMCO1 protein levels predicted poor disease-specific survival ($P = 0.0001$; Fig. 1E) and metastasis-free survival ($P < 0.0001$; Fig. 1F). Multivariate analysis additionally demonstrated that pT, mitotic rate and TMCO1 protein level significantly correlated to disease-specific survival; pT, nodal metastasis and TMCO1 protein level considerably correlated with metastasis-free survival (Table 1). These results suggest that low TMCO1 protein level confers an independent prognostic indicator in UBUC patients. Array comparison genomic hybridization (aCGH) was performed, as analyzed (40 UBUCs) in our previous study (25), and showed frequent DNA copy number gain at loci spanning *TMCO1* gene at 1q24.1 (9/40, 22.5%), excluding the possibility of *TMCO1* gene deletion in UBUC patients (Supplementary Fig. S1). Thus, downregulation of TMCO1 protein is an independent prognostic factor in UBUCs.

Changes in TMCO1 level alter cell cycle distribution, cell viability and proliferation, colony formation and modulate the AKT signaling pathway in vitro

The *TMCO1* mRNA levels were highly expressed in HUC, RT4 and J82 cells and low in BFTC905 cells (Fig. 2A). Additionally, TMCO1 protein levels were high in RT4 and J82 cells and low in BFTC905 (Fig. 2B). Therefore, BFTC905 cells were used for overexpression and RT4 and J82 cells were used for knockdown of the *TMCO1* gene for functional studies in vitro. No methylation in the *TMCO1* promoter region was found in RT4, T24, J82 cell lines, non-tumor urothelium (n = 8) and UBUCs with high (n = 7) and low (n = 7) TMCO1 protein levels (Supplementary Materials and Methods & Table S3). Exogenous expression of the *TMCO1* gene in BFTC905 cells resulted in stable expression of the TMCO1-HaloTag fusion protein (Fig. 2C); this stably expressed protein induced G_1 cell cycle arrest ($P < 0.05$) and decreased the number of cells in S phase ($P < 0.01$) (Fig. 2D) as well as suppressed cell viability ($P < 0.001$; Fig. 2E), cell proliferation ($P < 0.001$; Fig. 2F), and colony formation (Fig. 2G)/anchorage-independent cell growth ($P < 0.001$; Fig. 2H). Alternately, stable knockdown of the *TMCO1* gene in RT4 cells inhibited *TMCO1* mRNA ($P < 0.001$) and protein levels, induced cell cycle progression to S phase ($P < 0.001$), and increased cell viability ($P < 0.01$), cell proliferation ($P < 0.01$) and colony formation/anchorage-independent cell growth ($P < 0.001$) (Fig. 2I-2N). These findings suggest that *TMCO1* functions as a tumor suppressor by regulating cell cycle progression in vitro.

Stable exogenous expression of the *TMCO1* gene in BFTC905 cells notably upregulated the protein levels of the TMCO1-HaloTag, RB transcriptional corepressor 1 (RB1), TP53, pTP53(S15), cyclin dependent kinase inhibitor 1A (CDKN1A) and CDKN1B; however, *TMCO1* stable expression also downregulated cyclin D1 (CCND1), cyclin dependent kinase 4 (CDK4), CCNE1, and CDK2 protein levels (Fig. 2O), as well as reduced the following ratios: pCDKN1A(T145) (inactive form)/CDKN1A and pCDKN1B(T157)(inactive)/CDKN1B (0.26 and 0.25) (Fig. S2A). A declined

pCDKN1A(T145)/CDKN1A or pCDKN1B(T157)/CDKN1B ratio indicates an increase in the corresponding active form. Upregulation of nuclear TP53 and CDKN1A, rather than the cytosolic forms, accounted for the total TP53 and CDKN1A levels (Fig. 2P). However, *TP53* mRNA levels remained unchanged (NS; Supplementary Fig. S2B), suggesting that TMCO1 might stabilize TP53 at the protein level. Accordingly, the expression levels of MDM2, an E3 ubiquitin ligase of TP53, and its upstream regulators, AKT and pAKT1(S473) (26), were next examined. Substantial downregulation of pAKT1(S473), MDM2 and pMDM2(S166) proteins were found in *TMCO1*-overexpressed BFTC905 (Fig. 2Q).

Stable *TMCO1*-knockdown RT4 cells exhibited an opposite protein expression pattern compared to *TMCO1*-overexpressed BFTC905 cells (Fig. 2R). The ratios of pCDKN1A(T145) (inactive)/CDKN1A (shTMCO1#3: 0.70; shTMCO1#5: 0.89) and pCDKN1B(T157) (inactive)/CDKN1B (shTMCO1#3: 0.92; shTMCO1#5:0.92) were similar to the control (shLuc) (Fig. S2C). Nuclear TP53 and CDKN1A as well as nuclear and cytosolic CDKN1B were downregulated (Fig. 2S), yet *TP53* mRNA levels were upregulated ($P < 0.05$; Supplementary Fig. S2D). Further, treatment with a proteasome inhibitor, MG132, increased the abundance of the TP53 protein in the shLuc group compared to the DMSO control. MG132 further restored shTMCO1-suppressed TP53 protein levels in RT4 cells (Fig. 2T), reinforcing the observation that TMCO1 stabilizes TP53 at the protein level. Stable knockdown of the *TMCO1* gene in J82 cells showed similar results to *TMCO1*-knockdown RT4 cells, except the levels of phospho/inactive CDKN1A (shTMCO1#3: 1.89; shTMCO1#5: 2.42) and CDKN1B (shTMCO1#3: 1.76; shTMCO1#5: 1.67) were much higher than the shLuc control, implying that TMCO1 predominantly inhibits phospho/inactive CDKN1A and CDKN1B in J82 cells (Fig. S3A-S3G). Moreover, 5 cyclin-dependent kinase inhibitors, CDKN1C, CDKN2A, CDKN2B, CDKN2C and CDKN2D, were not consistently upregulated or downregulated after overexpression and knockdown of the *TMCO1* gene in BFTC905 and

RT4 cells, respectively (Supplementary Fig. S4).

To evaluate whether TMCO1-suppressed cell proliferation was AKT signaling-dependent, a constitutively active AKT1 plasmid, pHRIG-AKT1 (23), was co-transfected with the pTMCO1-HaloTag plasmid into BFTC905 cells. Exogenous constitutive expression of the active *AKT1* gene markedly downregulated *TMCO1*-induced levels of RB1, TP53, pTP53(S15), CDKN1A, and CDKN1B, while it upregulated the TMCO1-suppressed protein levels of pCDKN1A(T145), pCDKN1B(T157), CCND1, CDK4, CCNE1, CDK2, exogenous AKT1 and pAKT1(S473), MDM2, and pMDM2(S166) (Fig. 2U) as well as phospho/inactive CDKN1A and CDKN1B (Fig. S2A). Constitutively active AKT1 overexpression reinstated TMCO1-inhibited cell proliferation ($P < 0.001$; Fig. 2V). Therefore, TMCO1 suppresses cell proliferation by downregulating pAKT1(S473).

Alterations of the TMCO1 level affect cell migration and invasion in vitro

Stable overexpression of the *TMCO1* gene in BFTC905 cells suppressed cell migration and invasion ($P < 0.001$; Fig. 3A, 3B), with marked downregulation of CD44 and VIM protein levels (Fig. 3C). On the other hand, stable knockdown of the *TMCO1* gene in J82 cells enhanced cell migration and invasion ($P < 0.001$; Fig. 3D, 3E), with notable upregulation of CD44 and VIM protein levels (Fig. 3F). Stable knockdown of the *TMCO1* gene in RT4 cells exhibited similar phenotypes to J82 cells (Supplementary Fig. S5). Accordingly, TMCO1 downregulation induces cell migration and invasion in vitro.

TMCO1 recruits PHLPP2 to dephosphorylate pAKT1(S473) in vitro

Recently, a family of protein phosphatases (PH domain leucine rich repeat protein phosphatases, PHLPPs: PHLPP1 and PHLPP2) were discovered and found to directly dephosphorylate and inactivate AKT, thus introducing a new negative regulator of the

phosphatidylinositol-4,5-bisphosphate 3-kinase (PI3K) oncogenic pathway (22). Individually, PHLPPs dephosphorylate the S473 residue (22) and protein phosphatase 2 catalytic subunit alpha (PPP2CA) dephosphorylates the T308 residue (27) of AKT1. Since the TMCO1 protein contributes to the deactivation of AKT1, we first hypothesized that TMCO1 might regulate PHLPP1 or PHLPP2 protein expression. However, PHLPP1 or PHLPP2 protein level was not altered after TMCO1 overexpression in BFTC905, RT4 or J82 cells (Fig. 4A). A dose-course experiment was conducted in BFTC905 cells and 15 μM was found to be effective for a pan-PHLPP inhibitor, NSC117079 (Supplementary Fig. S6). In *TMCO1*-overexpressed BFTC905 cells, treatments with NSC117079 upregulated pAKT1(S473) compared to DMSO/pHaloTag (control) and DMSO/pTMCO1-HaloTag transfectants. Moreover, compared to NSC117079/pHaloTag, pAKT1(S473) was downregulated in NSC117079/pTMCO1-HaloTag transfectants (Fig. 4B). Hence, PHLPPs are indeed involved in TMCO1-mediated dephosphorylation of pAKT1(S473). Confocal immunocytochemistry insinuated that TMCO1 were predominately colocalized with PHLPP2 protein (Fig. 4C), while only somewhat colocalized with PHLPP1 (Supplementary Fig. S7) in BTFC905 and RT4 cells. Co-IPs additionally demonstrated that PHLPP2, rather than PHLPP1, interacted with TMCO1 in RT4 and J82 cells (Fig. 4D). These results suggested that TMCO1 recruits PHLPP2 to dephosphorylate pAKT1(S473) in UBUC-derived cells. Exogenous expression of both TMCO1 and PHLPP2 remarkably downregulated pAKT1(S473) protein level (Fig. 4E) and AKT activity (Fig. 4F) in BFTC905 cells compared to overexpression of either TMCO1 or PHLPP2 alone, indicating that TMCO1 recruits PHLPP2 to deactivate pAKT1(S473).

Mutagenesis on S60 of the TMCO1 protein releases *TMCO1*-suppressed cell cycle progression and revises the AKT1-MDM2-TP53 signaling pathway

The TMHMM Server (28) predicted that residues #32 to #89 of the TMCO1 protein might

reside in the cytoplasmic region (Fig. 5A). We therefore, constructed 3 plasmids containing TMCO1 with T33A, S60A and S84A mutations to evaluate whether these potential phosphorylation sites are critical for TMCO1 function. As shown in Fig. 5B, overexpression of the TMCO1(WT) or each mutant in BFTC905 cells notably upregulated TMCO1(WT)-, TMCO1(T33A)-, TMCO1(S60A)-, TMCO1(S84A)-HaloTag, pAKT1(S473), MDM2, pMDM2(S166), and downregulated TP53, pTP53(S15), and CDKN1A protein levels. Overexpression of TMCO1(S60A), but not other mutants, released TMCO1(WT)-induced G_1 cell cycle arrest (Fig. 5C), , and increased AKT1 activity (Fig. 5D) compared to TMCO1(WT) overexpression. Neither WT nor any other mutant affected the *TP53* mRNA level (NS; Fig. S2E). Accordingly, S60 in the TMCO1 protein was found to be critical for the expression and stability of pAKT1(S473), MDM2, pMDM2(S166), TP53, pTP53(S15), and CDKN1A proteins, and AKT activity.

Mouse xenograft models were further applied to evaluate the effect of TMCO1 in vivo. In NOD/SCID mice, xenografts of BFTC905 cells with TMCO1(WT) ($P = 0.007$) and TMCO1(S84A) ($P = 0.039$) overexpression showed smaller tumors compared to the control (HaloTag) after mice were sacrificed. When compared to the TMCO1(WT) group, the TMCO1(T33A) ($P = 0.036$) and TMCO1(S60A) ($P = 0.006$) groups exhibited larger tumors. The TMCO1(S60A) group possessed greater tumor mass than TMCO1(S84A) ($P = 0.035$) (Fig. 5E; Supplementary Fig. S8). Stable TMCO1(WT) overexpression induced a large area of necrosis and a much lower percentage of cancer components. Ki-67 was highly expressed in pTMCO1(T33A)- and pTMCO1(S60A)-HaloTag-expressing xenografts compared to pHaloTag xenografts (Fig. 5F), suggesting that TMCO1(S60A) and TMCO1(T33A) mutants particularly impair the growth inhibitory property of the TMCO1 protein in vivo. In HTB-33 epithelial cells (cervix, derived from metastatic site, omentum), TMCO1 functions as a tumor suppressor in vitro and in vivo (Supplementary Fig. S9), thus reinforcing our findings.

Discussion

In this study, we found that a high TMCO1 protein level could be an independent prognostic factor for disease-specific and metastasis-free survivals in a subset of UBUC patients. In addition, low TMCO1 protein levels correlated with aggressive tumor behaviors. We further identified that some patients (most were non-muscle invasive UBUCs, data not shown) with low TMCO1 protein levels showed long-term survival. Recent genomic and transcriptomic experiments indicated that non-muscle invasive UBUCs and carcinoma in situ (CIS)/high-grade muscle-invasive UBUCs have distinct mutation and gene expression profile (29). Low invasive properties might weaken the tumor suppressor role of TMCO1 in these patients. In vitro and xenograft mice models supported *TMCO1* as a tumor suppressor gene in vivo. Few studies have focused on understanding the biological functions of TMCO1. Using genome-wide mappings followed by candidate gene sequencing, homozygosity for a 2-bp deletion in the *TMCO1* gene in patients with a syndrome characterized by craniofacial dysmorphism, skeletal anomalies, and mental retardation were identified (30). Another genome-wide association investigation in several cohorts detected a single nucleotide polymorphism (rs4656461) locating approximately 6.5 Kb downstream of the *TMCO1* gene, which was associated with advanced primary open-angle glaucoma (POAG) and less-severe POAG (31). TMCO1 was recently reported to provide a protective mechanism to prevent overfilling of ER stores with Ca^{2+} ions (12). Therefore, this is the first study to describe that loss of TMCO1 expression contributes to tumorigenesis. Immunohistochemical analysis indicates that the TMCO1 protein was highly expressed in the cytoplasm and cell membrane of non-tumor urothelium and non-invasive urothelial carcinomas. Low TMCO1 protein levels can be traced back to low *TMCO1* mRNA, however, predesigned assays for quantification of CpG methylation spanning 8 CpG islands by pyrosequencing did not detect methylated sites

in 4 distinct UBUC-derived cell lines and UBUCs with low TMCO1 protein levels. Thus, the possibility that methylation in the promoter region caused low *TMCO1* transcription was excluded. In addition, no evidence of the *TMCO1* gene deletion was found from our previous aCGH data (25). Accordingly, the regulation of *TMCO1* mRNA and subsequent protein levels might be attributed to the activities of its transcriptional factors or other epigenetic modifications except methylation.

We further identified that TMCO1 inhibits cell cycle progression accompanied with alterations of pAKT1(S473), MDM2, pMDM2(S166), TP53, pTP53(S15) and nuclear TP53, and CDKN1A protein levels in distinct UBUC-derived cell lines. Based on the Cancer Genome Atlas (TCGA) project, a few pathways were consistently dysregulated in UBUCs, including TP53 and RB1 tumor suppressors, receptor tyrosine kinase (RTK)/related RAS viral (r-ras) oncogene homolog 2 (RRAS2) and the PI3K/AKT/mechanistic target of rapamycin (MTOR) pathways that affect cell proliferation and survival (32,33). Along with our findings in this study, constitutive overexpression of active AKT1 reset the expression levels of *TMCO1*-altered cell cycle regulators and cell proliferation. Thus, we hypothesized that TMCO1 might deactivate AKT and its downstream signaling pathways. *TP53* mRNA levels were inconsistently altered in *TMCO1*-overexpressed and -knockdown cells, reinforcing the finding that TMCO1 stabilizes TP53 at the protein level. There are three isoforms of AKTs. These isoforms are encoded by different genes but share a conserved domain structure consisting of an N-terminal pleckstrin homology domain, a kinase domain and a C-terminal regulatory domain containing a hydrophobic motif. AKT1 is ubiquitously expressed, AKT2 is primarily expressed in insulin-responsive tissues and AKT3 is highly expressed in brain and testes (34). Former studies in various epithelial cell lines revealed that PHLPP1 binds and dephosphorylates AKT2 and AKT3, but not AKT1, whereas PHLPP2 binds and dephosphorylates AKT1 and AKT3, but not AKT2 (22). Unfortunately, exogenous

459 expression and knockdown of the *TMCO1* gene in 3 distinct UBUC-derived cell lines were
460 not able to change the expression levels of PHLPP1 or PHLPP2 protein in our study. Since
461 TMCO1 is a transmembrane protein, its upregulation or downregulation might alter the
462 interactions with other proteins, including membranous and nonmembranous proteins, in
463 UBUC-derived cells. Meanwhile, we found that a pan PHLPP inhibitor, NSC117079, notably
464 augments endogenous as well as TMCO1-suppressed pAKT1(S473) levels in BFTC905 cells,
465 implicating PHLPPs in TMCO1-mediated pAKT1(S473) deactivation. Our
466 immunocytochemistry and co-IP data additionally signified that TMCO1 and PHLPP2
467 proteins colocalize and interact in vivo. Further, simultaneous overexpression of the *TMCO1*
468 and *PHLPP2* genes synergistically decreased pAKT1(S473) level and AKT1 activity
469 compared to overexpression of either the *TMCO1* or *PHLPP2* gene alone. Together, these
470 data support the concept that TMCO1 recruits PHLPP2 to dephosphorylate pAKT1(S473). In
471 a well-characterized mechanism, AKT downregulates TP53 protein level by enhancing
472 MDM2-mediated targeting of TP53 degradation (35). Under nonstress conditions, MDM2, an
473 E3 ligase of TP53, binds to TP53 and monoubiquitinates it prior to exporting TP53 to the
474 cytoplasm, where it is polyubiquitinated. AKT-dependent phosphorylation of MDM2 on S166
475 facilitates this export (36). Therefore, TMCO1-suppressed pMDM2(S166) radically
476 facilitated the stability of the TP53 protein. Moreover, phosphorylation on S15 of the TP53
477 protein, i.e., pTP53(S15), is necessary to mediate TP53-dependent transcription (especially
478 *CDKN1A*) and growth arrest (37). In parallel to this scenario, a novel tumor suppressor,
479 TMCO1 is uncovered and found to recruit PHLPP2 to dephosphorylate pAKT1(S473),
480 downregulate MDM2 and phospho/active pMDM2(S166), upregulate TP53 and
481 phospho/active/nuclear pTP53(S15) and inhibit cell proliferation.

482 In addition to TP53, we also found that TMCO1 upregulates nuclear CDKN1A, and
483 downregulates phospho/inactive CDKN1A and CDKN1B in BFTC905 and J82, but not RT4

cells. Indeed, it has long been known that the AKT oncogenic kinase functionally phosphorylates [pCDKN1A(T145); pCDKN1B(T157), (S187) and (T198)] and inactivates the nuclear CDKN1A and CDKN1B by causing cytoplasmic mislocalization (38). In addition, AKT-dependent phosphorylation of CDKN1A on T145 prevents the formation of a complex between CDKN1A and proliferating cell nuclear antigen (PCNA), decreases binding of CDKN1A to CDK2, and promotes the assembly of CCND1/CDK4 complex (39,40). Similarly, upon AKT activation, the appearance of pCDKN1B(T157/T198) precedes CDKN1B-CCND1-CDK4 assembly in early G_1 (41), thereby promoting cell cycle progression. In the cell cycle, the key regulators of the G_1/S transition are cyclin D-CDK4/6 and cyclin E-CDK2. The activities of these complexes are regulated by the TP53 checkpoint, the RB1 tumor suppressor, the INK4 family of proteins (CDKN2A/p16, CDKN2B/p15, CDKN2C/p18, CDKN2D/p19) and the Cip1/Kip1 family (CDKN1A and CDKN1B) (42). Our overexpression and knockdown experiments suggest that the TMCO1 protein specifically upregulated and downregulated Cip1/Kip1, but not INK4 proteins. *TMCO1*-suppressed cell proliferation might be partially CDKN1A- and/or CDKN1B-dependent, since TMCO1 positively regulated nuclear/active CDKN1A and CDKN1B protein levels in vitro. Knockdown of the *TMCO1* gene was not able to upregulate phospho/inactive CDKN1A and CDKN1B, implying that AKT1 might not be the only kinase to phosphorylate CDKN1A and CDKN1B. Although CDKN1A can be induced by both TP53-dependent and -independent mechanisms, our findings are compatible with either pathway.

Among three mutants disrupting potential phosphorylation sites in the cytoplasmic region, we revealed that overexpression of the TMCO1(S60A), but not TMCO1(T33A) or TMCO1(S84A), protein reverses TMCO1-mediated AKT activity to 85%; pAKT1(S473), pMDM2(S166), pTP53(S15), CDKN1A protein levels, and cell cycle arrest, suggesting that

S60 is a critical residue in maintaining functional TMCO1-AKT-TP53 regulation in vitro. To our surprise, xenografts showed that both TMCO1(T33A) and TMCO1(S60A) expressed high Ki-67 label and exhibited larger tumors compared to TMCO1(WT), indicating that TMCO1(T33A) might induce tumor growth via an AKT/MDM2/TP53/CDKN1A-independent pathway. Similar to TMCO1(WT), overexpression of the TMCO1(T33A), TMCO1(S60A) and TMCO1(S84A) did not change the *TP53* mRNA level, strengthening the finding that TMCO1 affects downstream tumor suppressors at the post-transcriptional and/or -translational level. Undeniably, transmembrane proteins constitute approximately 20-30% of fully sequenced proteome, and they are crucial for a wide variety of cellular functions (28). Protein phosphorylation is the most important, well-studied post-translation modification in eukaryotes and is involved in the regulation of several cellular processes, such as cell growth and differentiation, signal transduction and apoptosis (43-45). Phosphorylation usually occurs at S, T, tyrosine (Y) and histidine (H) residues in eukaryotic proteins; approximately 30-50% of proteins are presumed to be phosphorylated at some point (46). In transmembrane proteins, phosphorylation sites are located at the cytoplasmic region (47). In nocodazole-induced mitotic arrested HeLa cells, phosphorylation on the intracytoplasmic S60 of the TMCO1 protein was identified (48), supporting our observations.

In addition to cell cycle arrest, exogenous expression and knockdown of the *TMCO1* gene additionally inhibited and enhanced cell migration and invasion in vitro. The CD44 protein has several important physiological functions in cell-cell and cell-matrix interactions including proliferation, adhesion, migration, hematopoiesis, lymphocyte activation, homing and extravasation (49). Epithelial cell migration was recently reported to require the interaction between the VIM and keratin intermediated filaments (50). The downregulation and upregulation of CD44 and VIM protein levels, respectively, after overexpression and

knockdown of the *TMCO1* gene was also reported, thus strengthening the tumor suppressor roles of *TMCO1* in cell migration in vitro.

Overall, we demonstrate low TMCO1 protein levels in a subset of UBUCs with aggressive behaviors. In distinct UBUC-derived cell lines, TMCO1 expression inhibited cell proliferation by modulating the protein levels of pAKT1(S473), MDM2, pMDM2(S166), TP53, pTP53(S15), nuclear/active CDKN1A and CDKN1B, CD44 and VIM in combination with decreasing cell viability, proliferation, colony formation/anchorage-independent cell growth, cell migration and invasion. Additionally, TMCO1 was found to recruit PHLPP2 to dephosphorylate pAKT1(S473) and reduce AKT activity, and the intramembrane S60 residue of the TMCO1 protein was found to play a crucial role in this AKT-dependent pathway. Clinical associations, in vitro indications and xenografts serve robust evidence that the *TMCO1* gene is a novel tumor suppressor in UBUCs. Downregulation of the TMCO1 protein can be an adverse prognostic factor for inferior outcomes in UBUC patients.

Figure Legends

Figure 1. Downregulation of the TMCO1 protein predicts poor disease-specific and metastasis-free survivals. **(A)** A heatmap shows the data analysis from GSE32894 (GEO dataset), which identified that the *TMCO1* transcript is significantly downregulated (P = 0.0009) in muscle-invasive UBUC (blue bars). **(B)** The downregulation of the *TMCO1* transcript was also predictive of poor overall survival in an independent dataset (GSE31684, GEO, NCBI; P = 0.0425). **(C)** Quantitative RT-PCR validated that *TMCO1* transcripts were downregulated in UBUCs with high pT stage (informative n = 30) compared to those in normal and pTa-T1 tissues. **(D)** Immunohistochemistry in 295 UBUC specimens further demonstrated that TMCO1 protein levels were notably highly expressed in non-tumor urothelium and non-invasive urothelial carcinomas compared to those of muscle-invasive

559 urothelial carcinomas. One representative image of each group is shown. Moreover, a low
560 TMCO1 protein level is significantly predictive of poor disease-specific and metastasis-free
561 survivals **(E, F)**.
562
563 **Figure 2.** In vitro assay demonstrates that the *TMCO1* gene functions as a tumor suppressor
564 and inhibits the AKT signaling pathway in UBUC-derived cells. Quantitative RT-PCR and
565 immunoblot analysis showed that endogenous *TMCO1* mRNA was highly expressed in
566 normal human urothelial cells (HUC) compared to RT4, J82, BFTC905, BFTC909 and T24
567 cells **(A)**; TMCO1 protein level was low in BFTC905, but high in RT4 and J82 cells **(B)**.
568 Immunoblot, flow cytometric, 3-(4,5-dimethylthiazol-2-yl)-2,5-diphenyltetrazolium bromide
569 (MTT), 5-bromo-2'-deoxyuridine (BrdU) and soft agar assays, along with stable transfection
570 of the pCMV6-TMCO1 plasmid, showed that exogenous *TMCO1* expression in BFTC905
571 cells notably upregulated TMCO1-HaloTag fusion protein **(C)**, induced G_1 cell cycle arrest
572 and decreased cells in S phase **(D)** and inhibited cell viability **(E)**, cell proliferation **(F)**,
573 colony formation and anchorage-independent cell growth (7 days) **(G, H)**. Instead, stable
574 knockdown of the *TMCO1* gene with two distinct shRNAi clones in RT4 cells notably
575 downregulated *TMCO1* mRNA (quantitative RT-PCR) and protein levels **(I)**, decreased and
576 increased cells in G_1 and S phase, respectively **(J)** and enhanced cell viability **(K)**, cell
577 proliferation **(L)**, colony formation and anchorage-independent cell growth **(M, N)**.
578 Meanwhile, stable transfection of the pTMCO1-HaloTag plasmid into BFTC905 cells notably
579 upregulated RB1, TP53, pTP53(S15), CDKN1A and CDKN1B and downregulated CCND1,
580 CDK4, CCNE1 and CDK2 protein levels **(O)**. Nuclear/cytosolic fractionation and
581 immunoblotting further displayed that stable transfection of the pTMCO1-HaloTag plasmid
582 in BFTC905 cells markedly upregulated nuclear TP53 and CDKN1A, both nuclear and
583 cytosolic CDKN1B **(P)** and downregulated pAKT1(S473), MDM2 and pMDM2(S166)

584 protein levels **(Q)**. Alternatively, knockdown of the *TMCO1* gene with 2 distinct shTMCO1
585 clones in RT4 cells, markedly downregulated RB1, TP53, pTP53(S15), CDKN1A, CDKN1B,
586 and CDK4 and upregulated CCND1, CCNE1, pAKT1(S473), MDM2 and pMDM2(S166)
587 protein levels **(R)**. Nuclear TP53 and CDKN1A and both nuclear and cytosolic CDKN1B
588 were downregulated **(S)**. **(T)** In the shLuc group, treatment with a proteasome inhibitor
589 MG132 (1 μM, 24 h), increased the TP53 protein level compared to the DMSO control
590 (without MG132). After stable knockdown of the *TMCO1* gene in RT4 cells with 2 distinct
591 clones, and treatment with MG132 (1 μM, 24 h), TP53 protein levels were found to be
592 upregulated compared to cells without treatment. **(U)** Stable transfection of
593 pTMCO1-HaloTag and a constitutively active AKT1 (myr-AKT1) plasmid (pHRIG-AKT1)
594 into BFTC905 cells notably downregulated RB1, TP53, pTP53(S15), CDKN1A and
595 CDKN1B and upregulated pCDKN1A(T145), pCDKN1B(T157), CCND1, CDK4, CCNE1,
596 CDK2, exogenous pAKT1(S473), MDM2, and pMDM2(S166) protein levels compared to
597 the pTMCO1-HaloTag group. **(V)** BrdU assay further showed that constitutively active AKT1
598 increased cell proliferation compared to the control (transfection of pHaloTag) and the
599 pTMCO1-HaloTag-transfected groups. All experiments were conducted in triplicate, and
600 results are expressed as the mean ± SEM. For immunoblot analysis, one representative image
601 is shown; GAPDH served as a loading control; GAPDH and PARP1 were used as cytosolic
602 and nuclear control, respectively. Statistical significance: *, $P < 0.05$; **, $P < 0.01$; ***, $P <$
603 0.001.
604
605 **Figure 3.** Exogenous expression the *TMCO1* gene in BFTC905 cells suppresses, while
606 knockdown in J82 cells induces cell migration and invasion. Wound healing, transwell
607 migration, and transwell invasion assays showed that stable transfection of the
608 pTMCO1-HaloTag plasmid into BFTC905 cells repressed cell migration **(A)**. Transwell

609 migration (24 h) and transwell invasion (24 h) assays were subjected to cell counting **(B)**.
610 Immunoblot analysis indicated that CD44 and VIM protein levels were both markedly
611 downregulated **(C)**. On the other hand, stable knockdown of the *TMCO1* gene with two
612 distinct shRNAi clones, shTMCO1#3 and #5, in J82 cells induced cell migration and invasion
613 **(D, E)** and upregulated CD44 and VIM protein levels **(F)**. All experiments were performed in
614 triplicate, and results are expressed as the mean ± SEM. For immunoblot analysis, one
615 representative image is shown, and GAPDH served as a loading control. Statistical
616 significance: ***, $P < 0.001$.
617
618 **Figure 4.** TMCO1 recruits PHLPP2 to dephosphorylate pAKT1(S473) in UBUC-derived
619 cells. **(A)** Stable transfection of the pTMCO1-HaloTag plasmid into BFTC905 cells was not
620 able to upregulate PHLPP1 or PHLPP2 protein levels. Knockdown of the *TMCO1* gene with
621 2 distinct shTMCO1 clones in RT4 and J82 cells slightly upregulated PHLPP1 protein levels.
622 **(B)** BFTC905 cells (2×10^5) were stably transfected with pHaloTag or pTMCO1-HaloTag,
623 seeded overnight and starved in medium containing 0.1% fetal bovine serum for 2 h before
624 treatment with a pan-PHLPP inhibitor, NSC117079 (15 μM) for 35 min at 37°C. Immunoblot
625 analysis showed that NSC117079 notably increased pAKT1(S473) protein level in
626 pHaloTag-transfected cells compared to the control group (DMSO/HaloTag); NSC117079
627 upregulated pAKT1(S473) protein level in the pTMCO1-HaloTag-transfected cells compared
628 to pTMCO-HaloTag-transfected BFTC905 cells. **(C)** Confocal immunocytochemistry
629 demonstrated that TMCO1 and PHLPP2 proteins are colocalized (cell membrane and
630 cytoplasm) in BFTC905 and RT4 cells. **(D)** Co-immunoprecipitation using anti-PHLPP1
631 (αPHLPP1) or anti-PHLPP2 (αPHLPP2) antibodies and immunoblotting with anti-TMCO1
632 antibody showed that PHLPP2, but not PHLPP1, interacted with TMCO1 protein in RT4 and
633 J82 cells. **(E)** Immunoblot analysis revealed that transient transfection of the

pTMCO1-HaloTag or pcDNA3-HA-PHLPP2 plasmid into BFTC905 cells, notably increased the expression levels of TMCO1-HaloTag or HA-PHLPP2 fusion proteins, respectively, while this transient transfection markedly downregulated pAKT1(S473) protein levels. Co-transfection of pTMCO1-HaloTag and pcDNA3-HA-PHLPP2 plasmids into BFTC905 cells additionally reduced pAKT1(S473) protein level compared to transfection with either the pTMCO1-HaloTag or pcDNA3-HA-PHLPP2 plasmid alone. **(F)** AKT activity assay by immunoprecipitation with anti-AKT antibody and immunoblotting with anti-pGSK3A(S21) antibody showed that co-transfection of pTMCO1-HaloTag and pcDNA3-HA-PHLPP2 plasmids markedly reduced AKT activity compared to transfection with either the pTMCO1-HaloTag or pcDNA-HA-PHLPP2 plasmid alone. GSK3A served as a loading control. All experiments were performed in triplicate. For immunoblot analysis, one representative image is shown; GAPDH or pan-actin served as a loading control.

Figure 5. Mutagenesis on serine 60 of the TMCO1 protein to alanine [TMCO1(S60A)] releases TMCO1(wild type, WT)-induced G_1 cell cycle arrest along with modulation of the AKT-MDM2-TP53 axis in vitro and in vivo. **(A)** The TMHMM Server v. 2.0 predicted residues #32 to #89 as the intracytoplasmic region, which contains 6 serine/threonine residues. **(B)** The three mutants, T33A, S60A and S84A, constructed into the pHaloTag plasmid, and wild type (WT) were transfected into BFTC905 cells. Transient transfection of the pTMCO1(WT)-, pTMCO1(T33A)-, pTMCO1(S60A)- or pTMCO1(S84A)-HaloTag into BFTC905 cells downregulated pAKT1(S473), MDM2, and pMDM2(S166) and upregulated TP53, pTP53(S15), and CDKN1A, except for the pTMCO1(S60A)-HaloTag group. Compared to the pTMCO1(WT)-HaloTag group, pAKT1(S473), MDM2 and pMDM2(S166) were upregulated, while TP53, pTP53(S15) and CDKN1A protein levels were downregulated in pTMCO1(S60A)-, but not the pTMCO1(T33A)- and pTMCO1(S84A) groups. **(C)**

Transient transfection of the pTMCO1(WT)-HaloTag, pTMCO1(T33A) or pTMCO1(S84A) plasmid, but not pTMCO1(S60A), for 24 h induced G_1 cell cycle arrest and decreased the number of cells in S phase. **(D)** AKT activity assay using GSK3A as a substrate revealed that the transient transfection of the pTMCO1(WT)-, pTMCO1(T33A)-, pTMCO1(S60A)- and pTMCO1(S84A)-HaloTag plasmids into BFTC905 cells for 24 h downregulated AKT1 activities compared to control (transfection of the pHaloTag plasmid). However, transfection of the pTMCO1(S60A)-HaloTag retained higher AKT activity compared to other mutants. GSK3A served as a loading control. **(E)** The *TMCO1* gene was stably overexpressed by transfection of the pTMCO1-HaloTag plasmid into BFTC905 cells and was selected with G418. *TMCO1*-overexpressed cells (1.5×10^7) were mixed with matrigel and injected into flank sites of mice ($n = 8$ for each group). The average tumor volume of pHaloTag (control)-transfected BFTC905 xenografts was larger than pHaloTag(WT)- and pTMCO1(S84A)-HaloTag xenografts by the end of the animal experiments (Day 29; $P = 0.007$; $P = 0.039$). Both pTMCO1(T33A)- and pTMCO1(S60A)-HaloTag groups embraced large tumors, compared to the pHaloTag(WT) xenografts ($P = 0.036$; $P = 0.006$). The average tumor size of the pTMCO1(S60A)-HaloTag group was also larger than the pTMCO1(S84A)-HaloTag xenografts ($P = 0.035$). **(F)** Mice were sacrificed on day 29, control xenografts (cells carrying pHaloTag) displayed a carcinoma with high cellularity, while the *TMCO1*-overexpressing group (pTMCO1-HaloTag) showed large areas of necrosis and stromal hyalinization and a much lower percentage of cancer components. Exogenous expression of TMCO1 was confirmed in each group that was transfected with pTMCO1(WT)- or each plasmid with a specific mutant (inset of *Upper* panel). Labeling indices of Ki-67 were notably decreased in specimens from pTMCO1(WT)- and pTMCO1(S84A)-HaloTag xenografts compared to the pHaloTag control.

Disclosure of Potential Conflicts of Interest

No potential conflicts of interest were disclosed.

Authors' Contributions

Conception and design: CF Li, WJ Wu, YL Shiue

Development of methodology: CF Li, YL Shiue

Acquisition of data: CF Li, WR Wu, TC Chan, YH Wang

Analysis and interpretation of data: CF Li, YL Shiue

Writing, review and/or revision of the manuscript: CF Li, YL Shiue

Administrative, technical, or material support: WR Wu, TC Chan, YH Wang, LR Chen, BW Yeh, SS Liang

Study supervision: CF Li, WJ Wu, YL Shiue

Acknowledgments

The authors are grateful to the Biobank at Chi Mei Medical Center.

References

1. Eble JN, Sauter G, Epstein JI, Sesterhenn IA. World Health Organization Classification fo Tumour. Pathology and Genetics of Tumours of the Urinary System and Male Genital Organs. . Lyon: Interantional Agency for Research on Cancer (IARC) press 2004.
2. Aben KK, Witjes JA, Schoenberg MP, Hulsbergen-van de Kaa C, Verbeek AL, Kiemeney LA. Familial aggregation of urothelial cell carcinoma. Int J Cancer 2002;98(2):274-8.
3. Lichtenstein P, Holm NV, Verkasalo PK, Iliadou A, Kaprio J, Koskenvuo M, *et al.* Environmental and heritable factors in the causation of cancer--analyses of cohorts of twins from Sweden, Denmark, and Finland. N Engl J Med 2000;343(2):78-85 doi 10.1056/nejm200007133430201.
4. Hall RR, Parmar MK, Richards AB, Smith PH. Proposal for changes in cystoscopic

follow up of patients with bladder cancer and adjuvant intravesical chemotherapy. BMJ 1994;308(6923):257-60.

5. Shipley WU, Kaufman DS, Tester WJ, Pilepich MV, Sandler HM. Overview of bladder cancer trials in the Radiation Therapy Oncology Group. Cancer 2003;97(8 Suppl):2115-9 doi 10.1002/cncr.11282 [doi].

6. Urbanowicz RJ, Andrew AS, Karagas MR, Moore JH. Role of genetic heterogeneity and epistasis in bladder cancer susceptibility and outcome: a learning classifier system approach. Journal of the American Medical Informatics Association : JAMIA 2013;20(4):603-12 doi 10.1136/amiajnl-2012-001574.

7. Mitra AP, Hansel DE, Cote RJ. Prognostic value of cell-cycle regulation biomarkers in bladder cancer. Semin Oncol 2012;39(5):524-33 doi 10.1053/j.seminoncol.2012.08.008.

8. Volanis D, Papadopoulos G, Doumas K, Gkialas I, Delakas D. Molecular mechanisms in urinary bladder carcinogenesis. J BUON 2011;16(4):589-601.

9. Tang L, Zhang Y. Mitochondria are the primary target in isothiocyanate-induced apoptosis in human bladder cancer cells. Mol Cancer Ther 2005;4(8):1250-9 doi 10.1158/1535-7163.mct-05-0041.

10. Brown GR, Hem V, Katz KS, Ovetsky M, Wallin C, Ermolaeva O, *et al.* Gene: a gene-centered information resource at NCBI. Nucleic Acids Res 2015;43(Database issue):D36-42 doi 10.1093/nar/gku1055.

11. Dokmanovic-Chouinard M, Chung WK, Chevre JC, Watson E, Yonan J, Wiegand B, *et al.* Positional cloning of "Lisch-Like", a candidate modifier of susceptibility to type 2 diabetes in mice. PLoS Genet 2008;4(7):e1000137 doi 10.1371/journal.pgen.1000137.

12. Wang QC, Zheng Q, Tan H, Zhang B, Li X, Yang Y, *et al.* TMCO1 Is an ER Ca(2+) Load-Activated Ca(2+) Channel. Cell 2016;165(6):1454-66 doi 10.1016/j.cell.2016.04.051.

13. Iwamuro S, Saeki M, Kato S. Multi-ubiquitination of a nascent membrane protein produced in a rabbit reticulocyte lysate. J Biochem 1999;126(1):48-53.

14. Zhang Z, Mo D, Cong P, He Z, Ling F, Li A, *et al.* Molecular cloning, expression patterns and subcellular localization of porcine TMCO1 gene. Mol Biol Rep 2010;37(3):1611-8 doi 10.1007/s11033-009-9573-8.

15. Arinaminpathy Y, Khurana E, Engelman DM, Gerstein MB. Computational analysis of membrane proteins: the largest class of drug targets. Drug Discov Today 2009;14(23-24):1130-5 doi 10.1016/j.drudis.2009.08.006.

16. Chen YL, Uen YH, Li CF, Horng KC, Chen LR, Wu WR, *et al.* The E2F transcription factor 1 transactives stathmin 1 in hepatocellular carcinoma. Ann Surg Oncol 2013;20(12):4041-54 doi 10.1245/s10434-012-2519-8.

17. Tzeng CC, Liu HS, Li C, Jin YT, Chen RM, Yang WH, *et al.* Characterization of two urothelium cancer cell lines derived from a blackfoot disease endemic area in Taiwan. Anticancer Res 1996;16(4A):1797-804.
18. Tang Y, Simoneau AR, Xie J, Shahandeh B, Zi X. Effects of the kava chalcone flavokawain A differ in bladder cancer cells with wild-type versus mutant p53. Cancer Prev Res (Phila) 2008;1(6):439-51 doi 10.1158/1940-6207.capr-08-0165.
19. Cheng YT, Li YL, Wu JD, Long SB, Tzai TS, Tzeng CC, *et al.* Overexpression of MDM-2 mRNA and mutation of the p53 tumor suppressor gene in bladder carcinoma cell lines. Mol Carcinog 1995;13(3):173-81.
20. Markl ID, Jones PA. Presence and location of TP53 mutation determines pattern of CDKN2A/ARF pathway inactivation in bladder cancer. Cancer Res 1998;58(23):5348-53.
21. Li CF, Wu WJ, Wu WR, Liao YJ, Chen LR, Huang CN, *et al.* The cAMP responsive element binding protein 1 transactivates epithelial membrane protein 2, a potential tumor suppressor in the urinary bladder urothelial carcinoma. Oncotarget 2015;6(11):9220-39.
22. Brognard J, Sierecki E, Gao T, Newton AC. PHLPP and a second isoform, PHLPP2, differentially attenuate the amplitude of Akt signaling by regulating distinct Akt isoforms. Mol Cell 2007;25(6):917-31 doi 10.1016/j.molcel.2007.02.017.
23. Xie R, Cheng M, Li M, Xiong X, Daadi M, Sapolsky RM, *et al.* Akt isoforms differentially protect against stroke-induced neuronal injury by regulating mTOR activities. J Cereb Blood Flow Metab 2013;33(12):1875-85 doi 10.1038/jcbfm.2013.132.
24. Wei RJ, Lin SS, Wu WR, Chen LR, Li CF, Chen HD, *et al.* A microtubule inhibitor, ABT-751, induces autophagy and delays apoptosis in Huh-7 cells. Toxicol Appl Pharmacol 2016;311:88-98 doi 10.1016/j.taap.2016.09.021.
25. Wang YH, Wu WJ, Wang WJ, Huang HY, Li WM, Yeh BW, *et al.* CEBPD amplification and overexpression in urothelial carcinoma: a driver of tumor metastasis indicating adverse prognosis. Oncotarget 2015;6(31):31069-84 doi 10.18632/oncotarget.5209.
26. Ogawara Y, Kishishita S, Obata T, Isazawa Y, Suzuki T, Tanaka K, *et al.* Akt enhances Mdm2-mediated ubiquitination and degradation of p53. J Biol Chem 2002;277(24):21843-50 doi 10.1074/jbc.M109745200.
27. Gao T, Furnari F, Newton AC. PHLPP: a phosphatase that directly dephosphorylates Akt, promotes apoptosis, and suppresses tumor growth. Mol Cell 2005;18(1):13-24 doi 10.1016/j.molcel.2005.03.008.
28. Krogh A, Larsson B, von Heijne G, Sonnhammer EL. Predicting transmembrane protein topology with a hidden Markov model: application to complete genomes. J

Mol Biol 2001;305(3):567-80 doi 10.1006/jmbi.2000.4315.

29. Li CF, Wu WJ, Shiue YL. Advances in molecular genetics of early-stage urothelial carcinoma. Transl Cancer Res 2016;5(Suppl 6):S1126-30.

30. Xin B, Puffenberger EG, Turben S, Tan H, Zhou A, Wang H. Homozygous frameshift mutation in TMCO1 causes a syndrome with craniofacial dysmorphism, skeletal anomalies, and mental retardation. Proc Natl Acad Sci U S A 2010;107(1):258-63 doi 10.1073/pnas.0908457107.

31. Burdon KP, Macgregor S, Hewitt AW, Sharma S, Chidlow G, Mills RA, *et al.* Genome-wide association study identifies susceptibility loci for open angle glaucoma at TMCO1 and CDKN2B-AS1. Nat Genet 2011;43(6):574-8 doi 10.1038/ng.824.

32. Zhao M, He XL, Teng XD. Understanding the molecular pathogenesis and prognostics of bladder cancer: an overview. Chin J Cancer Res 2016;28(1):92-8 doi 10.3978/j.issn.1000-9604.2016.02.05.

33. Smolensky D, Rathore K, Cekanova M. Molecular targets in urothelial cancer: detection, treatment, and animal models of bladder cancer. Drug Des Devel Ther 2016;10:3305-22 doi 10.2147/dddt.s112113.

34. Hers I, Vincent EE, Tavare JM. Akt signalling in health and disease. Cell Signal 2011;23(10):1515-27 doi 10.1016/j.cellsig.2011.05.004.

35. Abraham AG, O'Neill E. PI3K/Akt-mediated regulation of p53 in cancer. Biochem Soc Trans 2014;42(4):798-803 doi 10.1042/bst20140070.

36. Lavin MF, Gueven N. The complexity of p53 stabilization and activation. Cell Death Differ 2006;13(6):941-50 doi 10.1038/sj.cdd.4401925.

37. Loughery J, Cox M, Smith LM, Meek DW. Critical role for p53-serine 15 phosphorylation in stimulating transactivation at p53-responsive promoters. Nucleic Acids Res 2014;42(12):7666-80 doi 10.1093/nar/gku501.

38. Blagosklonny MV. Are p27 and p21 cytoplasmic oncoproteins? Cell Cycle 2002;1(6):391-3 doi 10.4161/cc.1.6.262.

39. Li Y, Dowbenko D, Lasky LA. AKT/PKB phosphorylation of p21Cip/WAF1 enhances protein stability of p21Cip/WAF1 and promotes cell survival. J Biol Chem 2002;277(13):11352-61 doi 10.1074/jbc.M109062200.

40. Rossig L, Jadidi AS, Urbich C, Badorff C, Zeiher AM, Dimmeler S. Akt-dependent phosphorylation of p21(Cip1) regulates PCNA binding and proliferation of endothelial cells. Mol Cell Biol 2001;21(16):5644-57 doi 10.1128/mcb.21.16.5644-5657.2001.

41. Larrea MD, Liang J, Da Silva T, Hong F, Shao SH, Han K, *et al.* Phosphorylation of p27Kip1 regulates assembly and activation of cyclin D1-Cdk4. Mol Cell Biol 2008;28(20):6462-72 doi 10.1128/mcb.02300-07.

42. Bruyere C, Meijer L. Targeting cyclin-dependent kinases in anti-neoplastic therapy.

827 Curr Opin Cell Biol 2013;25(6):772-9 doi 10.1016/j.ceb.2013.08.004.
828 43. Pawson T, Scott JD. Protein phosphorylation in signaling--50 years and counting.
829 Trends Biochem Sci 2005;30(6):286-90 doi 10.1016/j.tibs.2005.04.013.
830 44. Wood CD, Thornton TM, Sabio G, Davis RA, Rincon M. Nuclear localization of p38
831 MAPK in response to DNA damage. Int J Biol Sci 2009;5(5):428-37.
832 45. Zhang J, Johnson GV. Tau protein is hyperphosphorylated in a site-specific manner in
833 apoptotic neuronal PC12 cells. J Neurochem 2000;75(6):2346-57.
834 46. Kalume DE, Molina H, Pandey A. Tackling the phosphoproteome: tools and strategies.
835 Curr Opin Chem Biol 2003;7(1):64-9.
836 47. Tsaousis GN, Bagos PG, Hamodrakas SJ. HMMpTM: improving transmembrane
837 protein topology prediction using phosphorylation and glycosylation site prediction.
838 Biochim Biophys Acta 2014;1844(2):316-22 doi 10.1016/j.bbapap.2013.11.001.
839 48. Dephoure N, Zhou C, Villen J, Beausoleil SA, Bakalarski CE, Elledge SJ, *et al.* A
840 quantitative atlas of mitotic phosphorylation. Proc Natl Acad Sci U S A
841 2008;105(31):10762-7 doi 10.1073/pnas.0805139105.
842 49. Naor D, Sionov RV, Ish-Shalom D. CD44: structure, function, and association with
843 the malignant process. Adv Cancer Res 1997;71:241-319.
844 50. Velez-delValle C, Marsch-Moreno M, Castro-Munozledo F, Galvan-Mendoza IJ,
845 Kuri-Harcuch W. Epithelial cell migration requires the interaction between the
846 vimentin and keratin intermediate filaments. Sci Rep 2016;6:24389 doi
847 10.1038/srep24389.

Figure-1

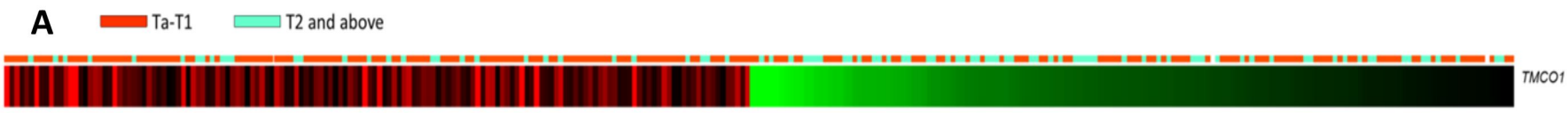

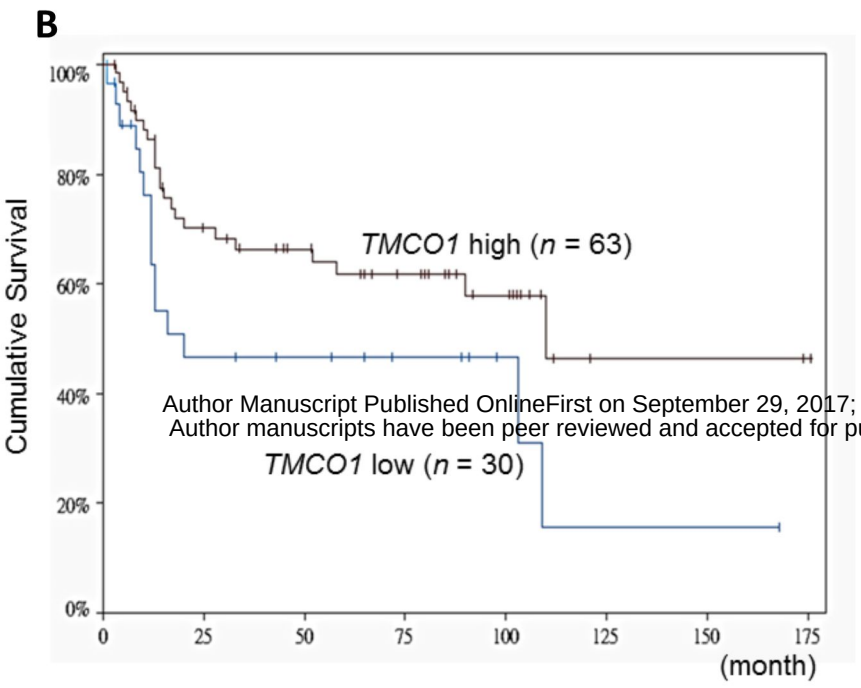

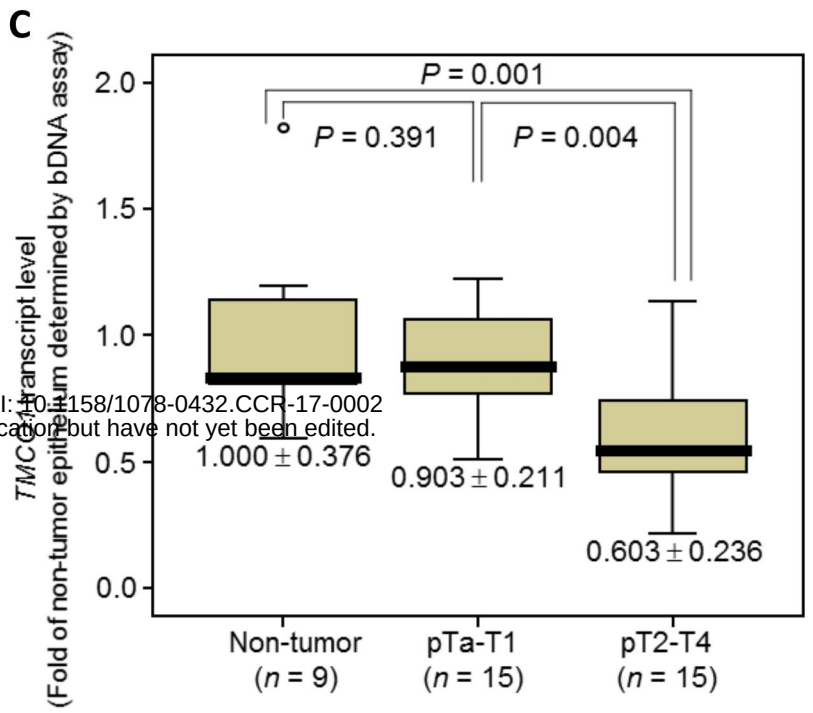

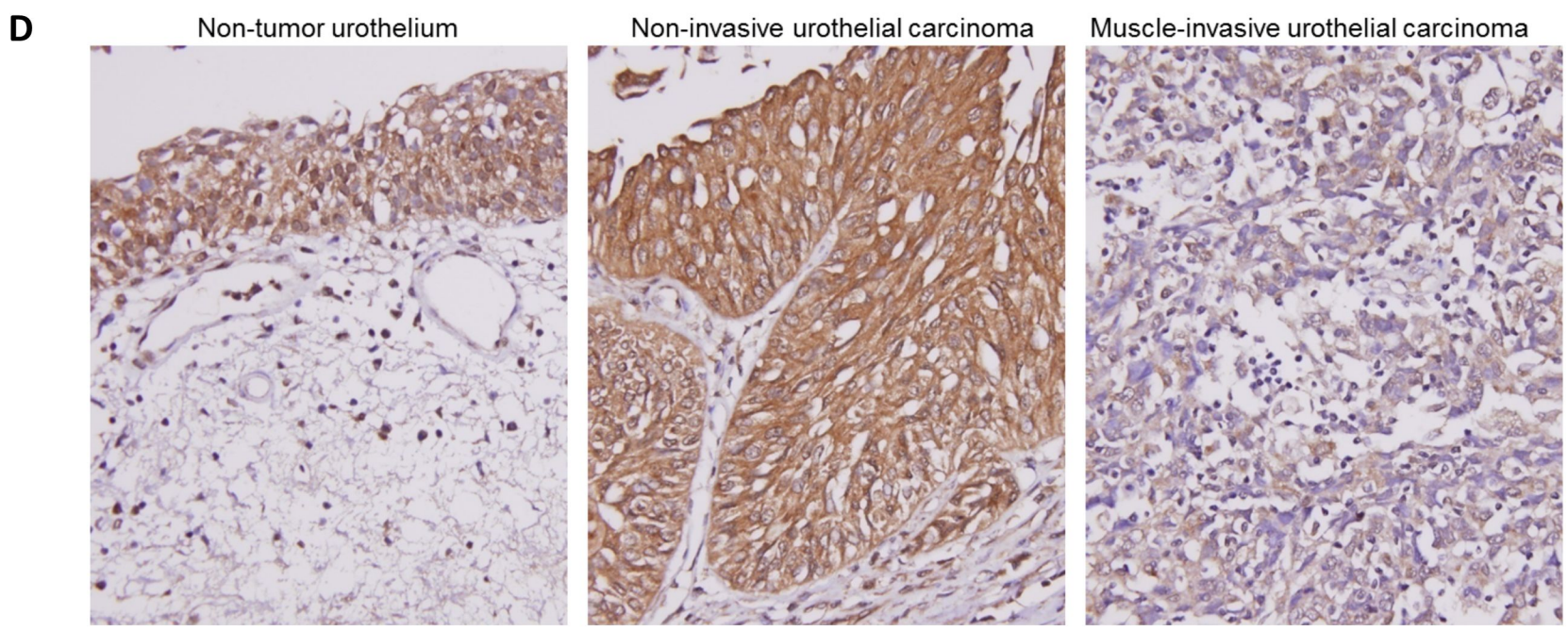

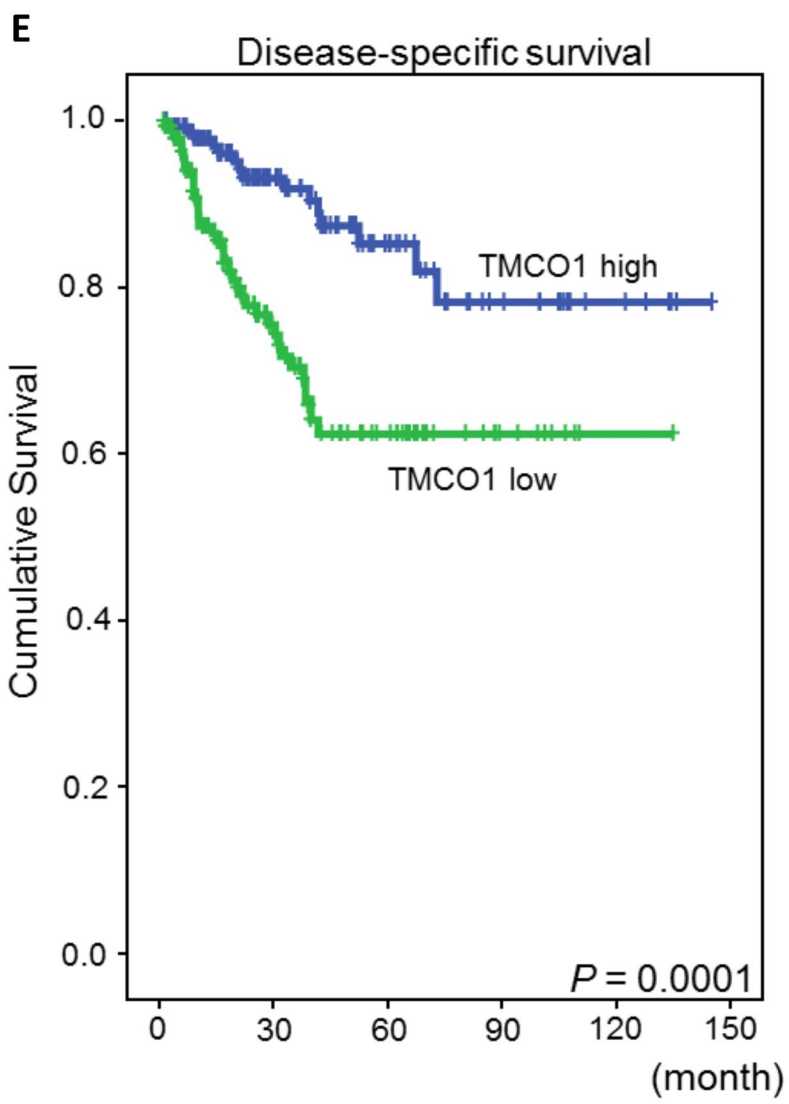

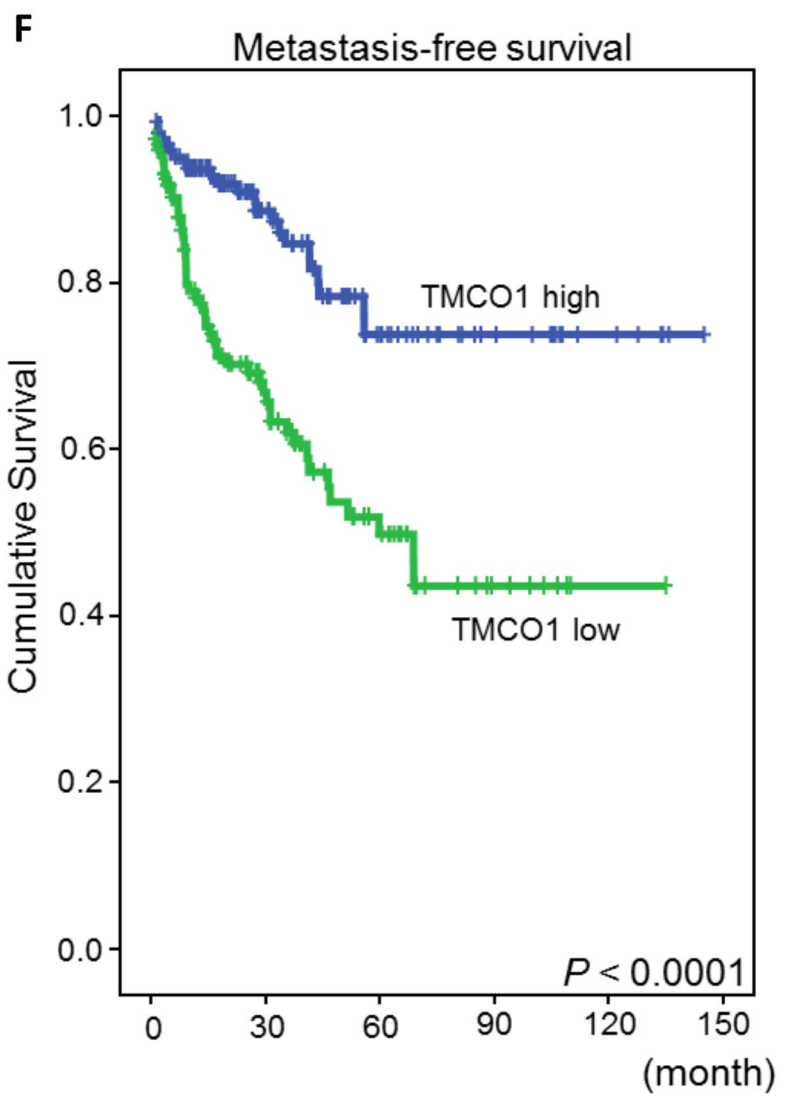

Figure-2

Author Manuscript Published OnlineFirst on September 29, 2017; DOI: 10.1158/1078-0432.CCR-17-0002
Author manuscripts have been peer reviewed and accepted for publication but have not yet been edited.

Figure-3

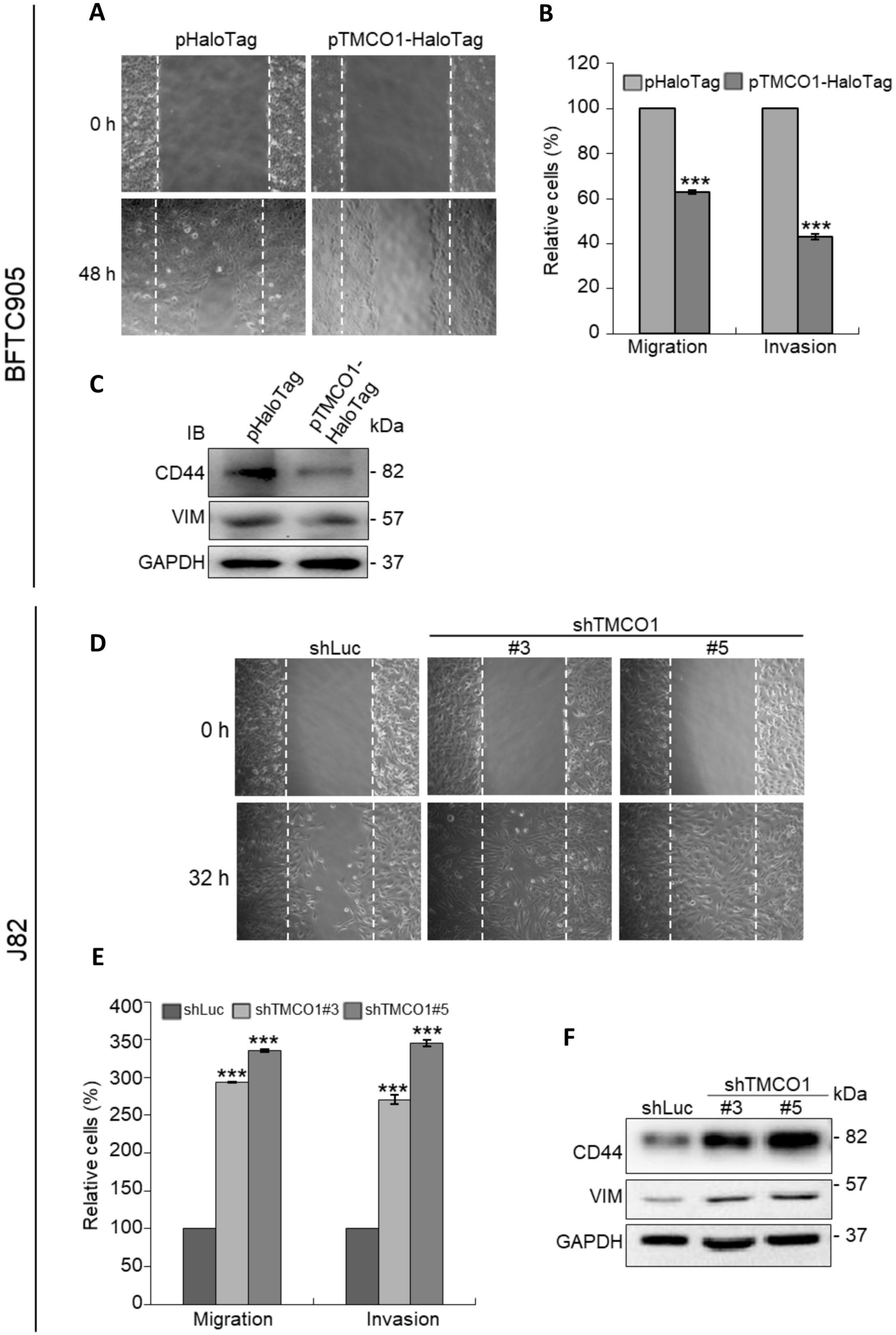

Author Manuscript Published OnlineFirst on September 29, 2017; DOI: 10.1158/1078-0432.CCR-17-0002
Author manuscripts have been peer reviewed and accepted for publication but have not yet been edited.

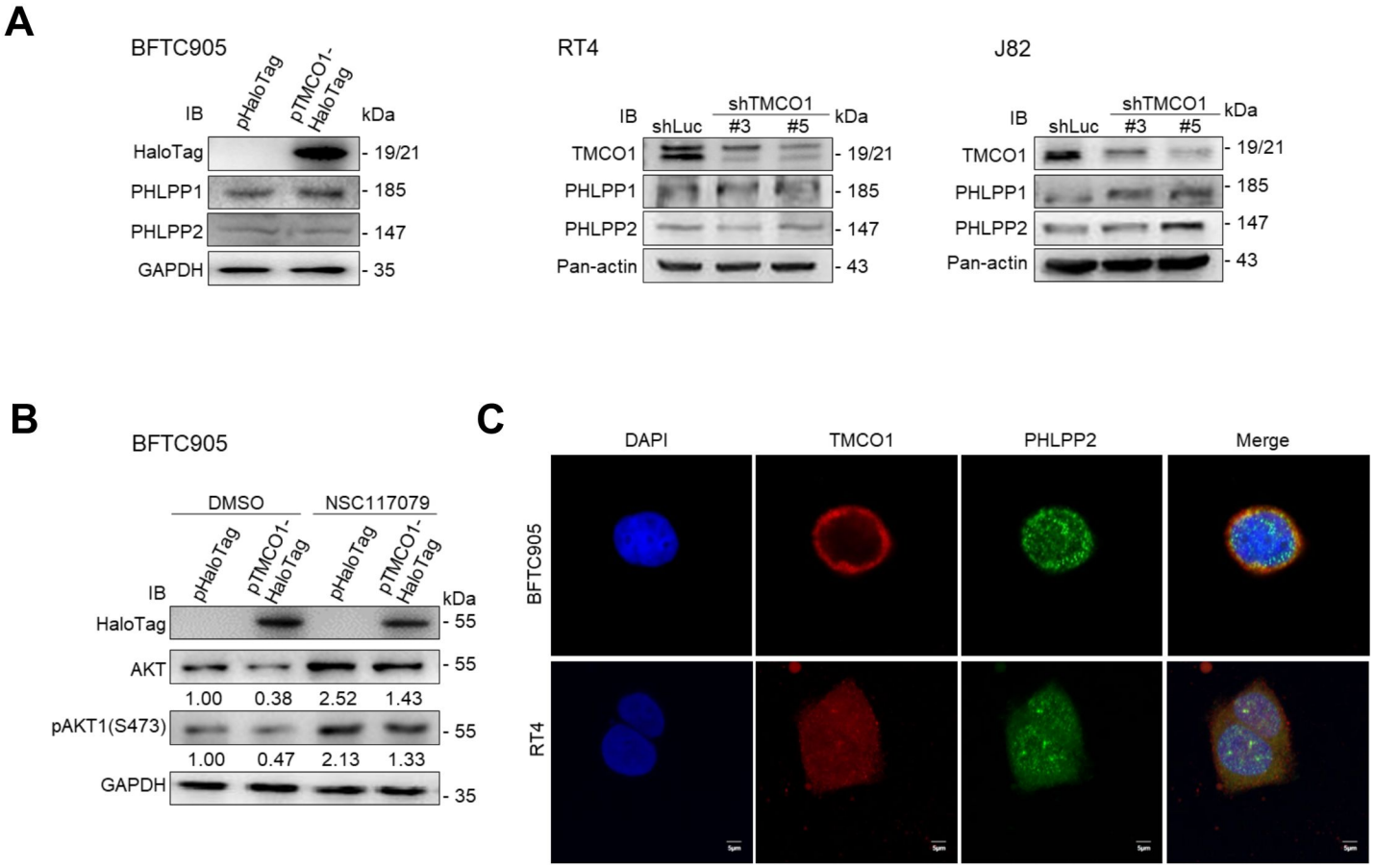

Figure-5

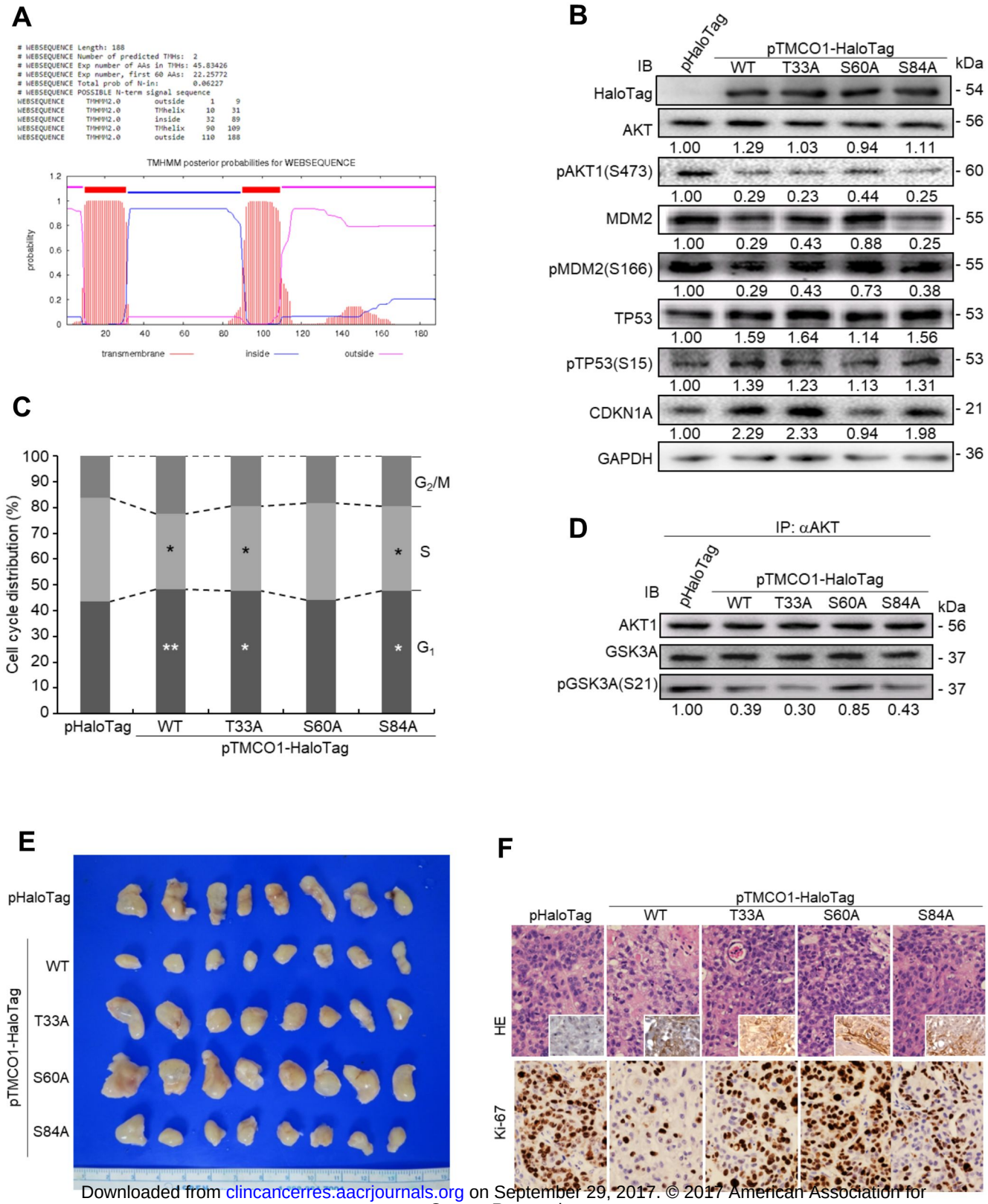

Table 1 Univariate log-rank and multivariate analyses for disease-specific and metastasis-free survivals in urinary bladder urothelial carcinoma

Parameter	Category	*n*	Disease-specific survival					Metastasis-free survival				
			Univariate analysis		Multivariate analysis			Univariate analysis		Multivariate analysis		
			n	*P* value	R.R.	95% C.I.	*P* value	*n*	*P* value	R.R.	95% C.I.	*P* value
Gender				0.4906					0.2745			-
	Male	216	41		-	-	-	61		-	-	
	Female	79	11		-	-	-	16		-	-	
Age (years)				0.1315					0.8786			-
	< 65	121	17		-	-	-	32		-	-	
	≥ 65	174	35		-	-	-	45		-	-	
Primary tumor (T)				**< 0.0001***			**< 0.001***		**< 0.0001***			**0.007***
	Ta	84	1		1	-		4		1	-	
	T1	88	9		4.971	0.545-45.368		23		3.928	1.159-13.313	
	T2-T4	123	42		23.327	2.709-200.847		50		6.460	1.921-21.720	
Nodal metastasis				**0.0001***			0.306		**< 0.0001***			**0.006***
	Negative (N0)	266	41		1	-		61		1	-	
	Positive (N1-N2)	29	11		1.448	0.713-2.942		16		2.365	1.275-4.386	
Histological grade				**0.0016***			0.827		**0.0008***			0.955
	Low	56	2		1	-		5		1	-	
	High	239	50		1.193	0.245-5.819		72		1.031	0.350-3.042	
Vascular invasion				**0.0010***			0.141		**< 0.0001***			0.796
	Absent	246	37		1	-		54		1	-	
	Present	49	15		0.593	0.296-1.189		23		1.083	0.592-1.983	
Perineural invasion				**< 0.0001***			0.055		**0.0003***			0.258
	Absent	275	44		1	-		67		1	-	
	Present	20	8		2.288	0.983-5.326		10		1.539	0.729-3.251	
Mitotic rate (per 10 high power fields)				**0.0001***			**0.045***		**0.0002***			0.098
	< 10	139	12		1	-		23		1	-	
	≥ 10	156	40		2.017	1.014-4.010		54		1.553	0.921-2.617	
TMCO1 protein level				**0.0001***			**0.036***		**< 0.0001***			**0.003***
	High	148	15		1	-		23		**1**	-	
	Low	147	37		1.945	1.046-3.620		54		**2.152**	**1.300-3.562**	

*, statistically significant; R.R., relative risk; C.I., confidence interval

AACR American Association for Cancer Research

Clinical Cancer Research

Transmembrane and coiled-coil domain 1 impairs the AKT signaling pathway in urinary bladder urothelial carcinoma: a characterization of a tumor suppressor

Chien-Feng Li, Wen-Ren Wu, Ti-Chun Chan, et al.

Clin Cancer Res Published OnlineFirst September 29, 2017.